Angewandte Chemie
Eine Zeitschrift der Gesellschaft Deutscher Chemiker

Supporting Information

69451 Weinheim, Germany

Dramatic Increase in the Oxygen Reduction Reaction for Platinum Cathodes from Tuning the Solvent Dielectric Constant**

Alessandro Fortunelli, William A. Goddard,* Yao Sha, Ted H. Yu, Luca Sementa, Giovanni Barcaro, and Oliviero Andreussi*

anie_201403264_sm_miscellaneous_information.pdf

Supporting Information

Here we provide more information on the energy barriers of the various ORR steps along the approach employed in the main text.

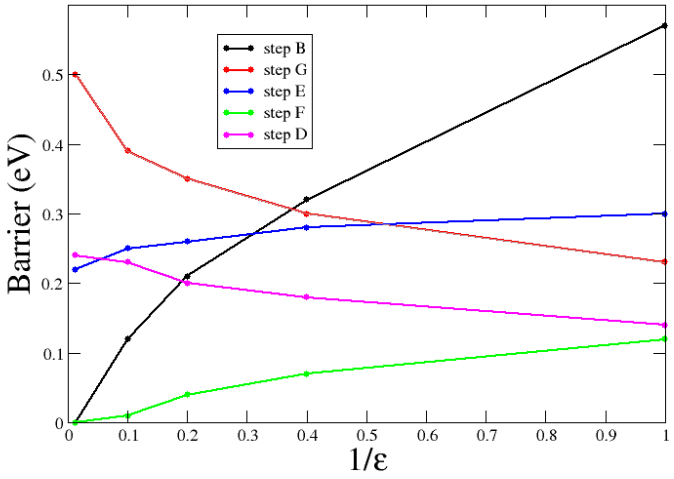

Figure S1. Energy barriers of the individual reaction steps of the ORR on Pt(111) as a function of the inverse of the dielectric constant of the solvent ε. The nomenclature of reaction steps is the same as in Figure1 of the main text.

Figure S1 reports the energy barriers of the individual reaction steps of the ORR on Pt(111) for the two competitive mechanisms: (a) O_2-diss-hydr (I), and (b) HOO-form-hydr (II), as a function of the inverse of the dielectric constant of the solvent ε. The nomenclature of reaction steps is the same as in Figure 1 of the main text. The values reported in Figure S1 have been used to produce Figure 2 of the main text.

Our main aim here is to validate with a different approach the predictions expounded in the main text and obtained by using the SeqQuest code[1] and the APBS continuum solvation model based on the Poisson-Boltzmann approximation[2-3]. In particular in this SI we compare the main text results with those obtained by using the PWscf code of the Quantum-ESPRESSO distribution[4] – which is a plane-wave periodic-boundary approach – to solve the Kohn-Sham DFT equations (thus a different numerical set-up), in conjunction with the self-consistent continuum solvation model (SCCS) proposed by Andreussi, Dabo and Marzari[5], and based on on previous work by Fattebert et al.[6-7].

We first check the energetics of the Oxygen Reduction Reaction (ORR) in the gas phase by locally optimizing all the configurations (intermediates) for the reaction steps (B-G) of the ORR on Pt(111) as depicted in Figure 1 of the main text, and calculating the corresponding activation energies. In the PWscf calculations unit cells using a slab made by four Pt layers, each containing 9 metal atoms (3x3 cells), are employed: the bottom two layers are frozen in the crystal positions by using the GGA-PBE equilibrium value of bulk Pt lattice constant (2.84 Å), whereas the top two layers are let free to relax together with the adsorbed species. We relax the local minima in a spin-unrestricted GGA-PBE framework using UltraSoft Pseudopotentials from the PWSCF library and cut-offs of 40 and 400 Ry on the wavefunctions and electronic density respectively, and by applying a Gaussian smearing of the one electron levels of 0.002 Ry. To locate the transition structures we use the Nudged Elastic Bands (NEB) approach[8-10] employing 7 images between the starting and final configurations. The geometry optimizations needed in the NEB approach use the same computational set-up as used to determine the local minima starting points of the NEB. It should be noted that, at variance with the APBS calculations reported in the main text, in the SCCS calculations we include salvation energy also in the geometry optimizations both for the reaction intermediate local minima and in the constrained minimizations needed in the NEB method. This is computationally much heavier but provides a really independent and rigorous test of our computational approach.

In Table S1, the energy differences and the energy barriers between the configurations shown in Figure 1 of the main text are reported and compared to the same values calculated by using the SeqQuest code[1] as used in the results reported in the main text. Except for steps (E) and (F) an overall excellent agreement is found between the two approaches. The discrepancies for steps (E) and (F) in Table S1 are due to the use of the experimental and DFT-predicted Pt lattice constant in the SeqQuest and PWscf models, respectively. Nevertheless, a fair agreement between the results of the two codes is apparent, especially for what concerns energy barriers, and gives us confidence to looking into what happens in solution.

Step	**Reaction**	**ΔE PWscf**	**ΔE SeqQuest**	**Barrier PWscf**	**Barrier SeqQuest**
B	**O_2 diss.**	-1.19	-1.10	0.55	0.57
C	**OH form.**	-0.23	-0.32	0.87	0.74
D	**H_2O form.**	-0.70	-0.79	0.06	0.14
E	**OOH form.**	-0.08	-0.32	0.53	0.30
F	**OOH diss.**	-0.36	-0.02	0.05	0.12

G	**O hydr.**	+0.18	+0.10	0.21	0.23

Table S1. Gas-phase energetics of the ORR steps (all energy values in eV). "Step" is the mechanistic step defined in Figure 1 of the main text, and "Reaction" is the acronym of the reaction it corresponds. **"**ΔE PWscf" is the reaction energy difference between products and reactants for the given step using the PWscf code, while "ΔE SeqQuest" is the corresponding values obtained with the SeqQuest code [1] (used for the main text results). Analogously, "Barrier PWscf" and "Barrier SeqQuest" are the reaction energy barriers of the given step using PWscf and SeqQuest codes, respectively.

Step	**Reaction**	**ΔE SCCS**	**ΔE APBS**	**Barrier SCCS**	**Barrier APBS**
B	**O_2 diss.**	-1.17	-2.32	0.00	0.00
C	**OH form.**	-0.39	+0.12	0.79	0.97
D	**H_2O form.**	-0.93	-0.48	0.29	0.24
E	**OOH form.**	-0.34	-0.29	0.43	0.22
F	**OOH diss.**	-0.30	-0.90	0.12	0.00
G	**O hydr.**	+0.40	+0.39	0.40	0.50

Table S2. Energetics of the ORR steps in water (all energy values in eV). All the quantities are defined as in Table S1, except that now "ΔE SCCS" and "ΔE APBS" refer to reaction energy differences in water in standard conditions calculated employing the PWscf/SCCS and SeqQuest/APBS approaches, respectively, while "Barrier SCCS" and "Barrier APBS" refer to the corresponding reaction energy barriers.

As a second stage, we thus compare the APBS predictions of the solvent effect on the energetics of the ORR with results obtained using the SCCS approach. The results of these calculations are reported in Table S2. From an inspection of this table, one can see that the two solvation models agree fairly well on the energy differences between the initial and final state of the OOH formation and the O hydration processes, whereas significant discrepancies can be noted for the other ORR steps. We then calculate the activation energies for all the reaction steps (B-G) using the NEB approach. The geometry optimizations needed in the NEB use the same computational set-up as used to determine the local minima starting an final points of the NEB. Results of such calculations are also reported in Table S2.

By comparing SCCS and APBS activation energies in Table S2, one finds an overall semi-quantitative agreement: the discrepancies between the two solvation models are never bigger than 0.21 eV. What is more important, in both approaches the preferred ORR mechanism on Pt(111) goes through the steps E-F-G-D. For the SCCS model the OOH formation step (E) is the rate determining step (rds) with a barrier of 0.43 eV: this value is similar to the energy barrier of the O hydration step (G) (0.50 eV) that is the rds according to the APBS model, whereas in the SCCS approach this step has a slightly smaller barrier of 0.40 eV. It can also

be noted that in the SCCS landscape step (E) becomes crucial for the ORR kinetics. While it will be interesting to validate which solvation approach is the more accurate by comparison with fully atomistic quantum simulations, the favourable agreement on activation energies between two completely different solvation models supports our predictions regarding the volcano curve for the ORR on Pt(111) as a function of the solvent dielectric constant.

References

[1] Schultz, P. SeqQuest code project; Sandia National Laboratories: Albuquerque, NM (http://www.cs.sandia.gov/~paschul/Quest/)

[2] Tannor, D.J.; Marten, B.; Murphy, R.; Friesner, R.A.; Sitkoff, D.; Nicholls, A.; Ringnalda, M.; Goddard, W.A.; Honig, B. Accurate First Principles Calculation of Molecular Charge-Distributions and Solvation Energies from Ab-Initio Quantum-Mechanics and Continuum Dielectric Theory *J. Am. Chem. Soc.* **1994**, 116, 11875 – 11882

[3] Baker, N.; Sept, D.; Joseph, S.; Holst, M.; McCammon, J. Electrostatics of Nanosystems: Application to Microtubules and the Ribosome. *Proc. Natl. Acad. Sci. U.S.A.* **2001**, 98, 10037-10041.

[4] Giannozzi, P.; et al. QUANTUM ESPRESSO: A Modular and Open-Source Software Project for Quantum Simulations of Materials. *J. Phys.: Condens. Matter*. **2009**, 21, 395502-1-395502-19

[5] Andreussi, O.; Dabo, I.; Marzari, N. Revised self-consistent continuum solvation in electronic-structure calculations *J. Chem. Phys.* **2012**, 136, 064102

[6] Scherlis, D. A.; Fattebert J. L.; Gygi, F.; Cococcioni, M.; Marzari, N. A unified electrostatic and cavitation model for first-principles molecular dynamics in solution *J. Chem. Phys.* **2006**, 124, 074103

[7] Fattebert J.L.; Gygi, F. Density functional theory for efficient ab initio molecular dynamics simulations in solution *J. Comput. Chem.* **2002**, *23*, 662 – 666

[8] Mills, G.; Jonsson, H. Quantum and Thermal Effects in H_2 Dissociative Adsorption - Evaluation of Free-Energy Barriers in Multidimensional Quantum-Systems *Phys. Rev. Lett.* **1994**, 72, 1124 – 1127

[9] Mills, G.; Jonsson, H.; Schenter, G.K. Reversible Work Transition-State Theory - Application to Dissociative Adsorption of Hydrogen. *Surf. Sci.* **1995**, 324, 305 – 337

[10] Henkelman, G.; Uberuaga, B.P.; Jonsson, H. A climbing image nudged elastic band method for finding saddle points and minimum energy paths *J. Chem. Phys.* **2000**, *113*, 9901 – 9904